

Novel full-human CD22-CAR therapy overcomes resistance to previous CD19/22-CAR regimens in ALL

Yue Tan

Chinese Academy of Medical Sciences Institute of Hematology and Blood Diseases Hospital

Haodong Cai

Tongji Hospital Department of Hematology

Chuo Li (✉ lichuo2018@163.com)

Peking Union Medical College Hospital

Biping Deng

Beijing Boren Hospital

Weiliang Song

Beijing Boren Hospital

Zhuojun Ling

Beijing Boren Hospital

Yongkun Yang

Nanjing Iaso Biotherapeutics Co.Ltd

Panpan Niu

Nanjing Iaso Biotherapeutics Co. Ltd

Guangrong Meng

Nanjing Iaso Biotherapeutics Co. Ltd

Wei Cheng

Nanjing Iaso Biotherapeutics Co. Ltd

Jinlong Xu

Beijing Boren Hospital

Jiajia Duan

Beijing Boren Hospital

Zelin Wang

Beijing Boren Hospital

Xinjian Yu

Beijing Boren Hospital

Xiaoming Feng

Chinese Academy of Medical Sciences Institute of Hematology and Blood Diseases Hospital

Jianfeng Zhou

Tongji Hospital Department of Hematology

Jing Pan

Beijing Boren Hospital

Research

Keywords: a potent full-human CD22-CAR T cell therapy, immunogenicity, B acute lymphoblastic leukemia

Posted Date: January 19th, 2021

DOI: <https://doi.org/10.21203/rs.3.rs-147858/v1>

License:  This work is licensed under a Creative Commons Attribution 4.0 International License. [Read Full License](#)

Abstract

Background

CD19- and/or CD22-targeted chimeric antigen receptor (CAR) T cells efficiently induced remission in patients with B acute lymphoblastic leukemia (B-ALL), but a considerable proportion of patients relapsed after both CD19- and CD22-CAR therapies associated with the loss or downregulation of target antigen. Re-infusions of the prior used CAR T cells were usually ineffective. In contrast to the frequent loss of CD19, low level of CD22 is usually present on leukemia cells post CAR therapy, suggesting that newly designed CD22-CAR therapies may be effective in these patients.

Methods

A yeast full-human single-chain variable fragment (scFv) library and a high-throughput NFAT reporter assay were utilized to screen several full-human CD22-CAR candidates; CD107 assay and in vitro cytotoxicity assay was used to evaluate the effector function of CAR T cells; membrane proteome assay was conducted to determine the specificity of the CAR toward the target antigen; a leukemia animal models was used to test the in vivo efficacy of CAR T cells. A phase I trial (ChiCTR2000028793) was conducted to assess the safety and effectiveness of CD22-CAR^{FH80} therapy in 8 children with B-ALL resistant to or relapsed after prior CD19- and CD22-CAR treatment.

Results

We identified a full-human CD22-CAR construct termed CD22CAR^{FH80} which could mediate superior anti-leukemia activity in vitro and in a leukemia animal model and had good specificity to the target antigen. Data from the trial showed that with CD22-CAR^{FH80} T-cell therapy, 6/8 (75%) patients including 2 who had CD22^{low} blasts achieved complete remission; 1 patient had a partial response. CAR T cells efficiently expanded in vivo, while the toxic effect is low in most patients. At a median follow-up of 5 months, 4/6 (57%) patients remained in remission.

Conclusions

Therapy with a newly invented CD22-CAR^{FH80} overcomes the resistance to prior versions of CD19- and CD22-CAR formats and elicits potent anti-leukemia responses with an acceptable safety profile, representing a promising salvage regimen for B-ALL that fails in prior CD19- and CD22-CAR treatments.

Trial registration

ClinicalTrials.gov: ChiCTR2000028793; registered 4 January, 2020. <http://www.chictr.org.cn/showproj.aspx?proj=47857>

Background

CD22-targeted chimeric antigen receptor (CD22-CAR) T cells efficiently induced remission in patients with B acute lymphoblastic leukemia (B-ALL) that lost CD19 expression¹⁻⁵, but a considerable proportion of patients still relapsed after CD22 CAR therapy⁵⁻⁸. In contrast to the commonly seen CD19⁻ relapse during CD19-CAR therapy, most patients who relapsed after CD22-CAR therapy retained various levels of CD22 expression on blasts, suggesting that re-treatment with CD22-CAR T cells may apply as a salvage regimen for them. But unfortunately, in our previous trials on a humanized CD22-CAR (termed CD22-CAR^{YK002}) T cell therapy, when we conducted a second CD22-CAR^{YK002} infusion in patients who relapsed after primary CD22-CAR^{YK002} treatment, most recipients displayed no or suboptimal anti-leukemia response and CAR T cell expansion (**Fig. 1a and b**, also see results).

The resistance to second CD22-CAR^{YK002} T cell infusion might be due to the immune response against primarily infused CD22-CAR^{YK002} transgene. Indeed, the immunogenicity of CAR was highlighted in recent clinical trials^{9,10}. Such anti-CAR responses may render subsequent CAR T cell infusions ineffective⁹. Although our CD22-CAR^{YK002} construct have been humanized, it might not always prevent generation of immunogenicity, as evidenced by a recent trial showing host immune response against the murine derived amino acid sequences in a humanized anti-CD22 antibody¹¹⁻¹³. Therefore, the pre-existing anti-CAR immunity in recipients might prevent reuse of CD22-CAR^{YK002} T cells. One way to avoid anti-CAR^{YK002} rejection is to adopt a distinctive CAR construct for second treatment. Furthermore, since the immunogenicity of full-human antibodies tends to be reduced compared with humanized or chimeric constructs¹³⁻¹⁶, the usage of a fully human derived CAR constructs might be a better strategy, which can not only avoid rejection by the pre-existing anti-CAR immunity, but also lower the risk of developing immune responses against the secondarily infused CAR T cells.

In our previous study and those of other groups, some patients relapsed after CD22-CAR T cell therapy carried CD22^{low} leukemia cells^{3,7}. There are cumulative evidences suggesting that leukemia cells with low level of CD22 expression are less sensitive to CAR activity^{3,7}; CD22 downregulation might represent a mechanism of relapse from primary CAR therapy or resistance to second CAR therapy. Therefore, to develop a CD22-CAR with superior activity against CD22^{low} target cells, may also improve the successful rate of CD22-CAR second treatment.

This study aims to develop a new full-human CD22-CAR construct for treating B-ALL patients who were refractory to or relapsed after prior CD19 and CD22-CAR therapies. We also attempt to develop a CAR which could mediate potent effect against B-ALL even if CD22 expression level is down-regulated. We used a full-human single chain fragment variant (scFv) yeast display library to screen a panel of full-human anti-CD22 scFvs which were

used to construct CD22-CAR variants, and identified a construct termed CD22-CAR^{FH80} with superior effector activity against CD22^{low} target cells. A phase I clinical trial was further conducted to evaluate safety and efficacy of CD22-CAR^{FH80} T cells in 8 children with CD22⁺ or CD22^{low} B-ALL that failed in prior CD19 and CD22-CAR therapies.

Methods

Screening of full-human anti-CD22 scFvs from a yeast display library

The full-human CD22-specific scFvs was screened from a yeast display human scFv library (Adimab, Lebanon). The DNA sequences encoding scFvs were generated from the heavy and light chain variable regions of various human antibodies by polymerase chain reaction (PCR), and cloned into an expression vector by homologous recombination, with the fusion to an activation domain (AD). The DNA sequence of the target peptide was cloned into another type of expression vector with fusion to a DNA binding domain (BD). A vector carrying a reporter gene with a specific DNA binding site were transduced into yeast cells. Then, the scFv-AD and Target-BD vectors were co-transformed into yeast cells¹⁷. If scFv-AD bound to the Target-BD, the Target-BD will bring the scFv-AD to the promoter to drive expression of the reporter gene. Yeast clones showing the reporter gene expression were selected, and the scFv sequences inside these clones were then identified.

In vitro and in vivo evaluation of different CD22-BBz variants

Nuclear factor of activated T cells (NFAT) reporter assay was conducted to test the activation of different CD22-BBz variants. The effector function and specificity of them was assessed via CD107a degranulation assay, cytotoxicity assay and membrane proteome array (MPA). Xenograft model and bioluminescence imaging was conducted to confirm the anti-leukemia effect of CD22-BBz 80 T cells in vivo. The details of these methods were in **Supplemental Method**.

Clinical trial design, patients, CAR T cell infusion, and clinical response assessment

A phase I trial of CD22-CAR^{FH80} T cell therapy was conducted in 8 refractory or relapsed (r/r) B-ALL pediatric patients who failed in prior humanized CD22-CAR^{YK-002} therapy, aged 5-12 years, between January 9, 2020 and July 16, 2020, at Beijing Boren Hospital. The study was approved by the institutional review board of Beijing Boren Hospital, and informed consent was obtained from individual patient in accordance with the Declaration of Helsinki. The trial was registered on Chinese Clinical Trial Registry/WHO International Clinical Trial Registry (ChiCTR2000028793). The baseline disease status was assessed immediately before enrollment (Details in **Table 1**). After patient enrollment, there was no further bridging chemotherapy before lymphodepleting procedure. The detailed procedure were detailed in **Supplemental Methods**.

Assessment and management of adverse events

Cytokine-release syndrome (CRS) and immune effector cell-associated neurotoxicity syndrome (ICANS) were graded by the most severe event according to ASTCT Consensus¹⁸. Specific organ toxicities were graded according to the National Cancer Institute Common Terminology Criteria for Adverse Events, CTCAE Version 5.0. The details of the managements of CRS and ICANS and other supportive cares are in **Supplemental Methods**.

Statistical analysis

Difference between two groups was analyzed by two-tailed, unpaired two-sample t-test. The comparison of the CRS and ICANS grade between CD22-CAR^{FH80} and CD22-CAR^{YK002} CAR T therapy in the same patient was analyzed by two-tailed Wilcoxon matched-pairs signed-rank test. All statistical analyses were performed using SPSS Statistics version 26, and P values of < 0.05 were considered significant.

Results

CD22-CAR^{YK002} T-cell second treatment was ineffective

Four B-ALL patients (A-D) who relapsed from CD22-CAR^{YK002} therapies had received a second infusion of CD22-CAR^{YK002} T cells (patient A, B were enrolled in ChiCTR-OIC-17013523; patient C, D were enrolled in ChiCTR-OIB-17013670) between May 8, 2018 and April 29, 2019 at Beijing Boren Hospital. The characteristics of these patients were shown in **Supplemental Table 1**. The treatment history of these patients was illustrated in **Fig. 1a**. CD22-CAR^{YK002} T cells were manufactured as previously described.⁵ After leukapheresis, patients received lymphodepleting chemotherapy before CD22 CAR^{YK002} T-cell infusion (day 0). The detailed infused dose of CD22-CAR^{YK002} T cells was detailed in **Supplemental Table 1**. Patients B, C and D displayed no response to the second infusion of CD22-CAR^{YK002} T cells; patient A had a transient complete response but quickly relapsed (**Fig. 1a**). The secondarily infused CD22-CAR^{YK002} T cells failed to expand as assessed by flow cytometry in all patients (**Fig. 1b**). The treatment overview was illustrated in **Fig. 1a**. These results collectively indicated that CD22-CAR^{YK002} second infusion were ineffective in patients who relapsed after primary CD22-CAR^{YK002} therapies.

Development of a novel full-human CD22-CAR^{FH80} with superior activity

Full-human anti-CD22 scFvs were screened from a full-human scFv yeast display library. The detailed procedure was described in Methods. To create a panel of CD22-BBz variants that harbored different anti-CD22 scFv fragments, the screened anti-CD22 scFvs were fused to the intracellular 4-1BB co-stimulatory and CD3ζ signaling domains, and further linked to epidermal growth factor receptor (tEGFR) with Thoseasigna virus 2A (T2A) to facilitate detection of CAR and elimination of CAR T cells when necessary (**Fig. 2a**). We next test the activation of Jurkat T cells transiently transduced with different CD22-BBz variants, in response to CD22^{high} Raji, CD22^{low} JVM-2 and CD22⁻ K562 cells (**Fig. 2b**) with NFAT reporter assay. The results showed that T cells transduced with CD22-BBz 80, 27, 36, 6 and 43 had the highest NFAT activation when co-cultured with Raji cells. However, CD22-BBz 6 and 43 also elicited marked NFAT activation in T cells without co-culturing with leukemia cells, probably owing to the off-target recognition or tonic signaling, and they were therefore excluded from further analyses. CD22-BBz 51, 15 and 23 had the low NFAT activation when co-cultured with Raji cells. Markedly, CD22-BBz 80, 27 and 36 also elicited substantial NFAT activation when co-cultured with JVM-2 cells, suggesting that these variants could trigger signaling even in response to target cells with low level of CD22 expression (**Fig. 2c and Supplementary Fig. 1**). CD22-BBz 80, 27 and 36 were thus defined as constructs which could transmit strong antigen-specific activation signals in T cells.

We then evaluated the effector function of primary T cells lentivirally transduced with CD22-BBz variants 80, 27, 36 and 51 (as a low NFAT activity control) via CD107a degranulation and cytotoxicity assay. High proportions of CD107a positivity (>30%) were detected in T cells bearing CD22-BBz 80, 27 and 36 when co-cultured with CD22^{high} Raji, Reh and Nalm6 cells. When co-cultured with the CD22^{low} JVM-2 cells, the CD107a expression was higher in T cell bearing CD22-BBz 80 and 36 than that bearing CD22-BBz 27. However, T cells bearing CD22-BBz 36 also showed considerable proportions of CD107a positivity when co-culturing with CD22⁻ K562, Jurkart and U266 cells and in medium alone, indicating nonspecific off-target effects. Lower proportions of CD107a positivity (<15%) were detected in T cells bearing CD22-BBz 51 when co-cultured with Reh, Nalm6 and JVM-2 cells. Three independent experiments from three different donors have been conducted with similar results (**Fig. 2d**). Cytotoxic assay indicated that T cells transduced with CD22-BBz 80 produced a slightly stronger cytolytic activity than CD22-BBz 27 and 36 T cells when co-cultured with Nalm6 and Reh cells (**Fig. 3a**). However, none of these CD22-BBz variants mediated obvious cytolytic activity against the JVM-2 cells, probably owing to a very refractory nature of JVM-2 cells, or the too low expression level of CD22 on JVM-2 cells. Nevertheless, CD22-BBz 80 was identified as a construct capable of eliciting the greatest T cell effector activity against target cells.

In concordance with the lack of cytolytic effect against the CD22⁻ cell lines, the membrane proteome array (MPA) showed that CD22-BBz 80 had a high specificity to the target antigen, suggesting a minimal risk of off-target effect if applied in therapy. (**Fig. 3b**). To confirm the anti-leukemia effect of CD22-BBz 80 T cells in vivo, NOD-Cg.Prkdc^{SCID}/IL-2Rgc^{null}/vst (NPG) mice were injected with 1×10^6 Nalm6-Luc cells 2 days before the treatment with different doses (0.5 and 2×10^6) of CD22-BBz 80 T cells and mock-transduced T cells. At the higher dose, CD22-BBz 80 T cells eliminated the Nalm6 tumors in two of the three mice treated, whereas at the lower dose, the tumor growth was significantly retarded despite that the tumor cells could not be completely eliminated (**Fig. 3c**). In contrast, mock-transduced T cells were ineffective against tumor growth. Thus, the full-human CD22-BBz 80 construct, which could mediate a potent and antigen-specific anti-leukemia activity, was termed CD22-CAR^{FH80} thereafter and used in the subsequent clinical study.

Patient enrollment and CD22-CAR^{FH80} T cell infusion

We then performed a phase I trial to assess the safety and efficacy of CD22-CAR^{FH80} T cells in 8 pediatric patients with advanced B-ALL that were refractory to or relapsed after prior humanized CD22-CAR^{YK002} treatment. The characteristics of enrolled patients were shown in **Table 1 and Supplementary Table 2**. The median age was 9 (range, 5-16) years. Six patients (75%) had hematological relapses as confirmed by bone marrow morphology, with a median marrow leukemia burden of 51% (range, 11% to 97%). Seven patients (87.5%) had detectable blasts in bone marrow by flow cytometry with a median percentage of 25% (range, 0.06% to 94.37%), including one with MRD. One patient (Pt 06) was MRD-negative in bone marrow but had diffused extramedullary disease involving right side posterior eyeball, chest wall, scapula, posterior sternum, pleura, hilum and accessory area.

Four patients (50%; Pt 01, 04, 06 and 08) had previously undergone allogeneic hematopoietic stem cell transplantation (allo-HSCT) including one (Pt 08) who had received twice HSCT. All patients (100%) were refractory (Pt 03 and 07) to or relapsed (Pt 01, 02, 04-06, 08) after prior versions of CD22-CAR therapies. Three patients (Pt 01, 04 and 08) relapsed after murine CD19-CAR T therapy, and were re-induced to remission with CD22-CAR^{YK002} T cells and subsequently bridged to HSCT but still had a relapse; 2 patients (Pt 02 and 05) relapsed after remission induced by sequential murine CD19-CAR and CD22-CAR^{YK002} therapy, and 1 of them (Pt 05) further received a humanized CD19-CAR T cell therapy but had no response; 2 patients (Pt 03 and 07) had a partial response to a tandem murine CD19-CAR/humanized CD22-CAR T cell therapy in an outer hospital, and 1 of them (Pt 03) further received infusion of CD22-CAR^{YK002} T cells in our hospital but had no response; 1 patient (Pt 06) repeatedly relapsed after murine CD19-CAR T cell therapy, CD22-CAR^{YK002} T cell therapy and HSCT, and then received humanized CD19-CAR therapy to achieve remission, but she finally developed diffused extramedullary disease one year later. The treatment histories of these patients were illustrated in **Fig. 4a**.

All patients had been confirmed to have positive CD22 expression on blasts by flow cytometry before enrollment. The CD22 expression level on blasts was not obviously reduced in 6 patients after prior CD22-CAR^{YK002} therapies, while patient 03 and 04 displayed lower CD22 expression on blasts than that before CD22-CAR^{YK002} treatments (**Fig. 4b and 4c**).

Before CD22-CAR^{FH80} T cell infusion, all patients received lymphodepleting chemotherapy with fludarabine (30 mg/m²/day) and cyclophosphamide (250 mg/m²/day). The median infused dose of CD22-CAR^{FH80} T cells was 1 (range, 0.68 to 9.4) × 10⁶ per kg body weight (/kg). Properties of the infused CAR T cells are shown in **Supplementary Table 3**.

CD22-CAR^{FH80} T cell therapeutic efficacy

The clinical response was evaluated on day 30 after CAR T cell infusion. Seven (87.5%) patients had a response. Six patients (75%) achieved MRD-negative complete remission, including 2 (Pt 03, 04) with low level of CD22 expression at enrollment. One patient (Pt 06) achieved partial remission in his extramudillary disease, as evidenced by an obvious reduction of the tumor mass behind his right eyeball and chest wall as detected by Magnetic Resonance Imaging (MRI) and Computed Tomography (CT) imaging on day 20 after infusion. The clinical responses to the therapy in individual patients were illustrated in **Fig. 5a**; images of patient 6 during treatment were shown in **Fig. 5b**.

The 7 responded patients were followed up with a median time of 6 months, and 4 patients (57%) were alive and disease-free until the cut-off date. The patients with a partial response (Pt 06) had his extramudillary lesions continuously shranked as evidence by MRI imaging on day 41, but the response could not be further monitored, since she succumbed to infection on day 42 after infusion. Of the 3 patients (Pt 02, 04 and 08) who received no further treatment, 2 (Pt 04 and 08) remained in remission status for 9 and 5 months, while 1 (Pt 02) had a CD22⁺ relapse and died of tumor progression 6 months after infusion. Three patients (Pt 01, 03 and 07) were bridged to HSCT as consolidation after CAR T cell infusion (the donors and pre-conditioning regimen were detailed in **Supplementary Table 4**), and among them two (Pt 01 and 07) remained in remission 10 and 5 months after infusion, and one (Pt 03) had a relapse with a mixture of CD22^{low} and CD22⁺ blasts 3 months after HSCT (**Fig. 5c**).

CD22-CAR^{FH80} T cell expansion *in vivo*

CD22-CAR^{FH80} T cells were readily detectable by flow cytometry in the peripheral blood of all patients. The expansion peaked from days 11 to 15 after infusion with a median value of 19.8 (range, 1.01-408) × 10⁶/L and 30 (range, 1-45) % among CD3⁺ T cells in the blood. The non-responding patient (Pt 05) had significantly lower peak CAR T cell expansion (1.01 × 10⁶/L; 1% among CD3⁺ T cells) than other patients, despite that her cultured CAR T cell viability (76.5%) and transduction efficiency (44%) and infused cell dose (3.49×10⁶/kg) were at intermediate to high levels among all patients. The reason for her poor CAR T cell expansion warrants further investigation. The CAR T cells were detectable by flow cytometry in the blood of 6/8 (75%) patients at day 30 after infusion (**Fig. 6a and 6b**). We did not routinely evaluate CAR T cell expansion beyond 30 days after infusion in patients who achieved complete remission and were discharged from our hospital. The details of CAR T cell expansion in individual patients were summarized in **Table 1** and **Supplementary Table 5**.

Since CD22-CAR T cells also eliminated normal B cells¹⁹, B cell aplasia and hypogammaglobulinemia could be used a reliable measurement of the active surveillance of CAR T cells²⁰. The 4 patients who achieved remission and received no further treatments all exhibited B cell aplasia and hypogammaglobulinemia until the observation end point (**Fig. 6c**), suggesting a prolonged persistence of CAR T cells. In the 3 patients who adopted HSCT after infusion, since the pre-conditioning regimen would eliminate CAR T cells, non-malignant B cells or serum immunoglobulin levels could not serve as a marker for evaluating CAR T cell status.

Adverse events and management, and serum cytokines

CRS occurred in 7/8 (87.5%) patients, including 6 with grade 1 CRS (75%) and 1 with grade 3 CRS (12.5%). The non-responding patient exhibited no signs of CRS, in accordance with his minimal CAR T cell expansion. The median time to onset was 3 days (range, 1 to 12 days), and the median duration was 10 days (range, 2 to 19 days). Fever was commonly observed in 6 patients, but other symptoms were rare (**Fig. 7a**). The six patients who experienced grade 1 CRS were given some supportive care including antipyretics and intravenous fluids, and their symptoms were relieved quickly. Patient 7 started to have a fever (< 40 °C) with hypoxia requiring low-flow nasal cannula (3 L/minute) at day 12, and received an intravenous injection of 80 mg tocilizumab, but she still developed grade 3 CRS from day 13 to 16 manifested as pulmonary edema and hypoxia requiring low-flow nasal cannula (6 L/minute). After intravenous injection of dexamethasone (10 mg/kg/d, from day 14 to 15), her CRS was reduced to grade 1 from day 16 to 19, and fully resolved at day 20.

Neurologic toxicities occurred in 2/8 (25%) patients. One patient (Pt 03) developed grade 2 ICANS from day 5 manifested as mild abnormality in orientation, naming, following command, writing and attention, accompanied with fever and resolved on day 6 after giving antipyretics. The other patient (Pt 07) developed grade 3 ICANS from day 14, manifested as seizure and positive neck rigidity, and loss of consciousness. In this patient, 0.1 g of benzodiazepine and 30 mg of diazepam were respectively intramuscularly and intravenously injected once as acute management, and mannitol at 2.5 ml/kg/dose and furosemide at 1 mg/kg/dose were intravenously administered from day 13 to 19 to reduce intracranial pressure. Dexamethasone was intrathecally administered once at 5 mg at day 14, and intravenously used at 10 mg/kg/d from day 14 to 15, and subsequently administered at 7.5 mg/kg/d until all symptoms were relieved. The detailed manifestations and managements of CRS, ICANS, and other toxicities suspected to be related to CAR T cells were shown in **Fig. 7a** and **7b** and **Supplementary Table 6**. We further compared the severity of CRS and ICANS between CD22-CAR^{FH80} and the prior CD22-CAR^{YK002} therapies in the same individual patients, but found no significant difference (P=0.414 and 0.285, **Supplementary Fig. 2**).

Despite the monthly immunoglobulin replacement, one patient (Pt 06) died from infection. She only transiently experienced a mild CRS manifested as fever but quickly resolved. On day 37 after infusion, she developed a high fever, and . On day 41, MRI examination indicated an intracranial infection, and she started to have symptoms of seizure and quickly progressed to unconscious despite the usage of antibiotics and finally died **Supplementary Fig. 3**). A perianal abscess was found after she was in a coma, so her sepsis was suspected to derive from the perianal infection.

Serum cytokines indicative of systemic inflammation including IL-6, IL-10, TNF- α , sCD25 and ferritin were elevated after infusion and reached peak levels around 9 days (range, 6-21) after infusion (**Fig. 7c**). Most patients had dramatic increases of IL-6, ferritin and sCD25, while only a small proportion of the patients had obvious increase of TNF- α and IL-10. The patient (Pt 07) who developed grade 3 CRS and ICANS showed the highest peak levels of IL-6, ferritin and sCD25.

Discussion

In this study, we developed a new version of full-human CD22-CAR^{FH80} construct with superior activity against CD22^{low} target cells, and in a following clinical trial CD22-CAR^{FH80} T cells induced MRD-negative remission in 75% (6/8) patients. Efficient expansion of the CD22-CAR^{FH80} T cells was observed in all responded patients. The high response rate with CD22-CAR^{FH80} therapy implicates that there is no overt cross immunogenicity between CD22-CAR^{FH80} and prior infused CD22-CAR^{YK002} transgenes. Markedly, CD22-CAR^{FH80} therapy was even effective in 2 patients with CD22^{low} blasts, while in the two patients who relapsed after CD22-CAR^{FH80} therapy only CD22⁻ blasts were majorly present, indicating that CD22^{low} leukemia cells have been efficiently removed by CD22-CAR^{FH80} T cells.

The good tolerability of patients to CD22-CAR^{FH80} therapy is supported by that low grade CRS and ICANS occurred in 7/8 (87.5%) patients, despite that 4/8 (50%) had high leukemia burdens (> 50% blasts with bone marrow biopsy), which is associated with increased likelihood of severe CRS¹⁷. Only 1 patient with an intermediate leukemia burden (50%) in BM but no blasts in CSF developed grade 3 CRS and ICANS. One patient (Pt 6) started to have infection at day 37 after infusion, and died of intracranial infection at 2 months, but she only transiently experienced grade 1 CRS manifested as moderate fever from at day 1–2 after infusion, accompanied with a moderate elevation of serum cytokine levels, but had no neurologic manifestations. So, her late infection was unlikely to be directly related to the CAR T cells.

Anti-CAR immune responses may reduce CAR T cell persistent duration to dampen long-term efficacy^{9–10,21–22}. In this study, 3 patients were bridged to HSCT after remission induced by CD22-CAR^{FH80} T cells. Since the conditioning procedure before HSCT would eliminate CAR T cells, the long-term immunogenicity and persistent capacity of CAR T cells cannot be evaluated in them. Four patients without HSCT consolidation remained in B cell aplasia and hypogammaglobulinemia until the cut-off date, indicating the continued presence of CD22-CAR^{FH80} T cells, but the follow-up time is not long enough, and the immunogenicity and persistent capability of CD22-CAR^{FH80} needs to be further investigated.

Previous version of CD22-CAR^{YK002} was also very efficient in inducing remission in B-ALL patients as indicated in our previous study⁵. Whether CD22-CAR^{FH80} outperforms CD22-CAR^{YK002} in persistence or long-term efficacy against B-ALL still warrants future study. In addition, a CD22-CAR containing a full-human scFv, termed m971, generated from a human phage library have produced convincing activity in B-ALL patients in a phase I trial⁷. Our CD22-CAR^{FH80} will add into this line of CD22-CAR products for improving outcome of ALL patients. The distinctive features and values of different CD22-CAR therapies warrant future study.

Conclusions

In summary, this study successfully developed a novel full-human CD22-CAR^{FH80} construct with potent activity against CD22^{low} B-ALL, and established the safety and effectiveness of CD22-CAR^{FH80} T cell therapy with a phase 1 trial in patients who have failed from prior CD19 and CD22-CAR T cell treatment. The power of this therapy is based on its minimal cross-immunogenicity with prior versions of CD22 CAR products and capacity to treat patients with CD22^{low} leukemia. Despite that future phase 2/3 studies are needed to verify and optimize this therapy, our study indicates an important value of CD22-CAR^{FH80} for advanced ALL patients that are insensitive to prior versions of CAR therapies.

Abbreviations

CAR: chimeric antigen receptor; B-ALL: B acute lymphoblastic leukemia; scFv: single chain fragment variant; NFAT: Nuclear factor of activated T cells; CRS: Cytokine-release syndrome; ICANS: immune effector cell-associated neurotoxicity syndrome; allo-HSCT: allogenic hematopoietic stem cell transplantation; MRI: Magnetic Resonance Imaging; CT: Computed Tomography; MPA: membrane proteome array

Declarations

Acknowledgments

We thank the patients and their families who participated in this study. And we also thank all physicians, nurse, and other patient care providers involved in the care of these patients.

Author contributions

Y.T., C.L. and J.P. contributed to clinical data collection, data analyses, data interpretation. H.C. performed most preclinical experiments and analyses. B.D., Y.Y., P.N., G.M. and W.C. contributed to the CAR T cell manufacture. J.P., Z.L., W.S., J.X., J.D. and Z.W. contributed to the clinical protocol. X.Y. was responsible for leukemic cell immunophenotyping. Y.T. conducted statistical analyses. Y.T., C.L., J.P. and X.F. wrote the manuscript. J.P., and X.F. designed the clinical trial, directed the study and had final responsibility to submit for publication. The authors read and approved the final manuscript.

Funding

This work was supported by the National Key R&D Program of China (2019YFA0110200), the Tianjin Science Funds for Distinguished Young Scholars (17JCJQJC45800), the CAMS Innovation Fund for Medical Sciences (CIFMS, 2016-I2M-1-003), and the Non-profit Central Research Institute Fund of Chinese Academy of Medical Sciences (2018PT32034).

Availability of data and materials

All data associated with this study are present in the paper or the Supplementary Materials.

Ethics approval and consent to participate

All samples were used after by the Institutional Review Board and informed consent was obtained from each individual in strict accordance with the principles in Declaration of Helsinki.

Consent for publication

Not applicable.

Competing interests

Adimab, LLC, a global company contribute to the discovery and optimization of fully human monoclonal and bispecific antibodies, holds a patent on full-human non-immune monoclonal antibody yeast display library. Y.Y., P.N., G.M. and W.C. are also employees of Nanjing Iaso Biotherapeutics Co. Ltd., whose potential product was studied in this work. The remaining authors declare that they have no conflict of interest.

References

1. Uy N, Nadeau M, Stahl M, Zeidan AM. Inotuzumab ozogamicin in the treatment of relapsed/refractory acute B cell lymphoblastic leukemia. *J Blood Med.* 2018; 9: 67-74.
2. Raponi S, De Propis MS, Intoppa S, et al. Flow cytometric study of potential target antigens (CD19, CD20, CD22, CD33) for antibody-based immunotherapy in acute lymphoblastic leukemia: analysis of 552 cases. *Leuk Lymphoma.* 2011; 52: 1098-1107.
3. Haso W, Lee DW, Shah NN, et al. Anti-CD22-chimeric antigen receptors targeting B-cell precursor acute lymphoblastic leukemia. *Blood.* 2013; 121: 1165-74.
4. Shah NN, Stevenson MS, Yuan CM, et al. Characterization of CD22 expression in acute lymphoblastic leukemia. *Pediatr Blood Cancer.* 2015; 62: 964-969.
5. Pan J, Niu Q, Deng B, et al. CD22 CAR T-cell therapy in refractory or relapsed B acute lymphoblastic leukemia. *Leukemia.* 2019; 33: 2854-2866.
6. Shah NN, Highfill SL, Shalabi H, et al. CD4/CD8 T-Cell Selection Affects Chimeric Antigen Receptor (CAR) T-Cell Potency and Toxicity: Updated Results From a Phase I Anti-CD22 CAR T-Cell Trial. *J Clin Oncol.* 2020; 38: 1938-1950.
7. Fry TJ, Shah NN, Orentas RJ, et al. CD22-targeted CAR T cells induce remission in B-ALL that is naive or resistant to CD19-targeted CAR immunotherapy. *Nat Med.* 2018; 24: 20-28.
8. Pan J, Tan Y, Deng B, et al. Frequent occurrence of CD19-negative relapse after CD19 CAR T and consolidation therapy in 14 TP53-mutated r/r B-ALL children. *Leukemia.* 2020; 10: 1038.
9. Turtle CJ, Hanafi LA, Berger C, et al. Immunotherapy of non-Hodgkin's lymphoma with a defined ratio of CD8+and CD4+CD19-specific chimeric antigen receptor-modified T cells. *Sci Transl Med.* 2016; 8: 355ra116.
10. Maus MV, Haas AR, Beatty GL, et al. T cells expressing chimeric antigen receptors can cause anaphylaxis in humans. *Cancer Immunol.* 2013; 1: 26-31.
11. Leonard JP, Goldenberg Preclinical and clinical evaluation of epratuzumab (anti-CD22 IgG) in B-cell malignancies. *Oncogene.* 2007; 26: 3704-3713.
12. Kreitman RJ, Wilson WH, Bergeron K, et al. Efficacy of the anti-CD22 recombinant immunotoxin BL22 in chemotherapy-resistant hairy-cell leukemia. *N Engl J Med.* 2001; 345: 241-247.
13. Xiao XD, Ho M, Zhu ZY, et al. Identification and characterization of fully human anti-CD22 monoclonal antibodies. *mAbs.* 2009; 1: 297-303.
14. Lanitis E, Poussin M, Hagemann IS, et al. Redirected antitumor activity of primary human lymphocytes transduced with a fully human anti-mesothelin chimeric receptor. *Mol Ther.* 2012; 20: 633-643.

15. Song DG, Ye Q, Poussin M, et al. A fully human chimeric antigen receptor with potent activity against cancer cells but reduced risk for off-tumor toxicity. *Oncotarget*. 2015; 6: 21533-21546.
16. Alonso CV, Martín DS, Compte M, et al. CAR bodies: Human Antibodies Against Cell Surface Tumor Antigens Selected From Repertoires Displayed on T Cell Chimeric Antigen Receptors. *Mol Ther Nucleic Acids*. 2013; 2: e93.
17. Gietz D, St Jean A, Woods RA, Schiestl RH. Improved method for high efficiency transformation of intact yeast cells. *Nucleic Acids Res*. 1992; 20: 1425.
18. Lee DW, Santomasso BD, Locke FL, et al. ASTCT Consensus Grading for Cytokine Release Syndrome and Neurologic Toxicity Associated with Immune Effector Cells. *Biol Blood Marrow Transplant*. 2019; 25: 625-638.
19. Maude SL, Frey N, Shaw PA, et al. Chimeric antigen receptor T cells for sustained remissions in leukemia. *N Engl J Med*. 2014; 371: 1507-1517.
20. Kalos M, Levine BL, Porter DL, et al. T cells with chimeric antigen receptors have potent antitumor effects and can establish memory in patients with advanced leukemia. *Sci Transl Med*. 2011; 3: 95ra73.
21. Lamers CH, Willemsen R, Elzakker P, et al. Immune responses to transgene and retroviral vector in patients treated with ex vivo-engineered T cells. *Blood*. 2011; 117: 72-82.
22. Lam N, Trinklein ND, Buelow B, et al. Anti-BCMA chimeric antigen receptors with fully human heavy-chain-only antigen recognition domains. *Nat Commun*. 2020; 11: 283.

Tables

Table 1. Baseline characteristics, CAR T cell dose, clinical response and adverse events of individual patients

Patient No./Gender/Age	Prior therapy period (months)/lines	Number of prior CAR T therapies ^a	Number of HSCTs	EMDs	CAR T cells infused ($\times 10^6/\text{kg}$)	Response to CAR	Post-CAR Treatment	Outcome	CRS	Neurological toxicity	Therapy (30 days)
1/F/16	72	2	1	None	1.43	CR/MRD-	HSCT	CCR/11	Grade 1	-	
2/F/7	49	3	-	None	0.96	CR/MRD-	-	R/Death/6	Grade 1	-	
3/M/6	24	3	-	None	2.5	CR/MRD-	HSCT	R/4	Grade 1	Grade 2	
4/M/7	50	3	1	None	1.0	CR/MRD-	-	CCR/9	Grade 1	-	
5/F/5	27	3	-	None	3.49	NR	-	NR	-	-	
6/F/10	44	5	1	Diffused	9.4	PR	-	Death/2	Grade 1	-	
7/F/11	66	2	-	None	0.68	CR/MRD-	HSCT	CCR/6	Grade 3	Grade 3	
8/F/12	36	2	2	None	0.2	CR/MRD-	-	CCR/5	Grade 1	-	

F, female; M, male; EMD, extramedullary disease; MRD, negative minimal residual disease by flow cytometry; CCR, continued complete remission; CR, complete remission; NR, no response; PR, partial response; R, relapse; CRS, cytokine release symptom; HSCT, allogeneic hematopoietic stem cell transplantation; -, None. ^aAll previous CAR T therapies and response for each patient are detailed in Supplementary table 1.

Figures

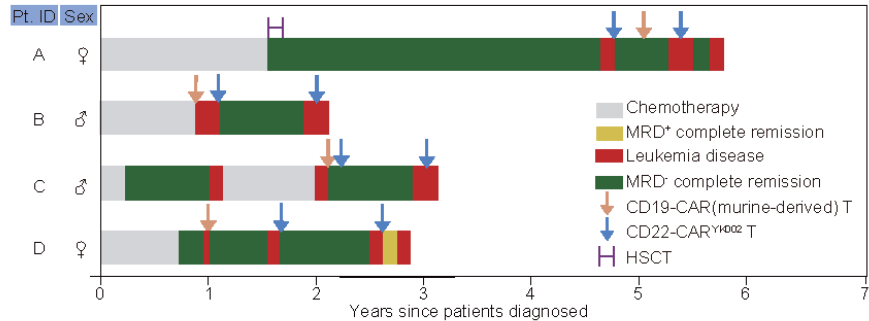
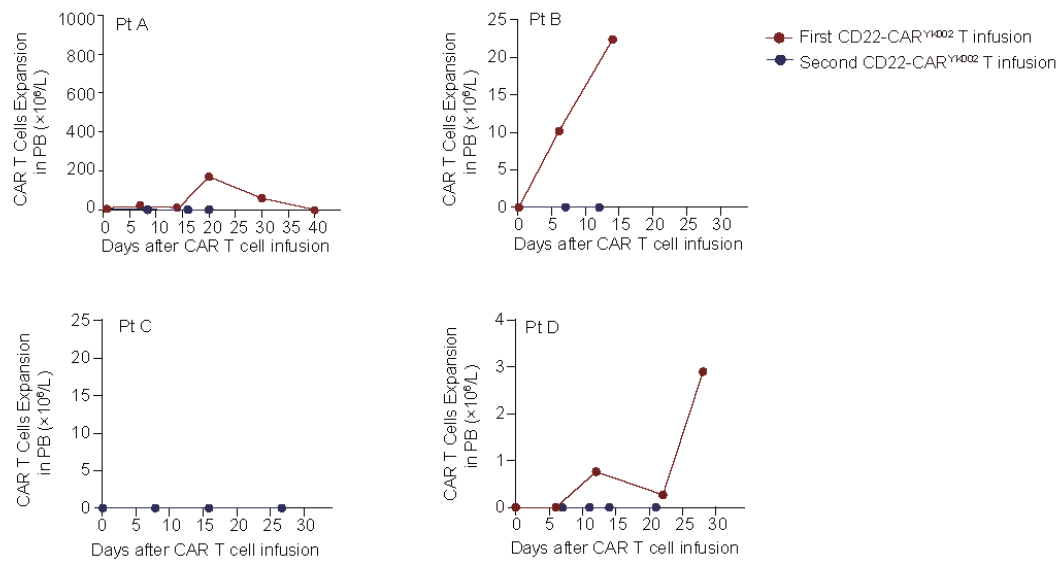
A**B**

Figure 1

Figure 1

CD22-CARYK002 T-cell second treatment was ineffective in 4 patients who relapsed after primary CD22-CARYK002 therapies a, Swimmer plot illustrating the treatment history of 4 patients relapsed from prior therapy with CD22-CARYK002 T cells, and the clinical response after a second CD22-CARYK002 T cells re-infusion. Patient A achieved complete remission after second infusion of CD22-CARYK002 T cells, but she relapsed after one month; patient B and C had no response to second CD22-CARYK002 T cells infusion; patient D achieved minimal residual disease-positive remission in response to second CD22-CARYK002 T cells infusion at day 15, but soon relapsed at day 30. HSCT, hematopoietic stem cell transplantation; MRD, minimal residual disease. b, Absolute numbers of CAR T cells detected by flow cytometry in the peripheral blood from two patients after the first and second infusion of CD22-CARYK002 T cells. No patients exhibited no detectable expansion of secondly infused CD22-CARYK002 T cells, as assessed by flow cytometry.

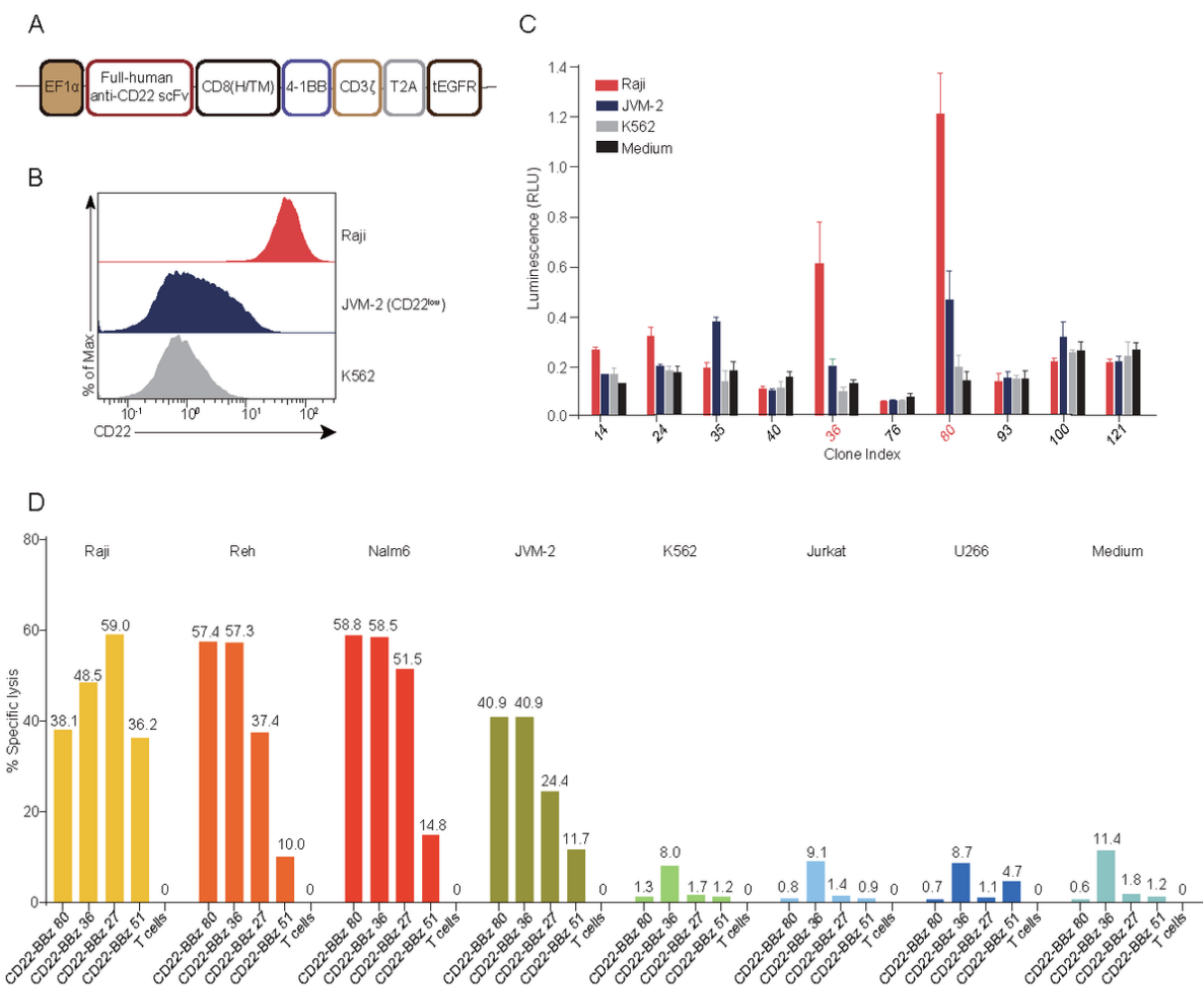


Figure 2

Figure 2

Development of a novel full-human CD22-CARFH80 construct with superior anti-leukemia activity a, Schematic of the recombinant lentiviral vectors encoding the full-human CD22-BBz variants. The expression of CAR transgene is under the control of the elongation factor 1a promoter. CD8 (H/TM), CD8a hinge and transmembrane domains; EGFR, epidermal growth factor receptor, T2A, Thoseaasigna virus 2A. b, Histogram of CD22 expression on Raji, JVM-2, and K562 cells, determined by flow cytometry. c, Nuclear factor of activated T cells (NFAT) reporter assay in T cells transduced with different CD22-BBz variants, after co-culturing with CD22high Raji, CD22low JVM-2 and CD22- K562 cells, or cultured in medium alone in triplicates. d, Bar chart showing CD107a expression in specific CD22-BBz T cell clones after co-culturing with CD22high Raji, Nalm6, Reh cells, CD22low JVM-2, and CD22- K562, Jurkat and U266 cells, as determined by flow cytometry. CD107a degranulation rates were calculated as the percentages of CD107a+ cells among CAR+CD8+ T cells and indicated above each bar.

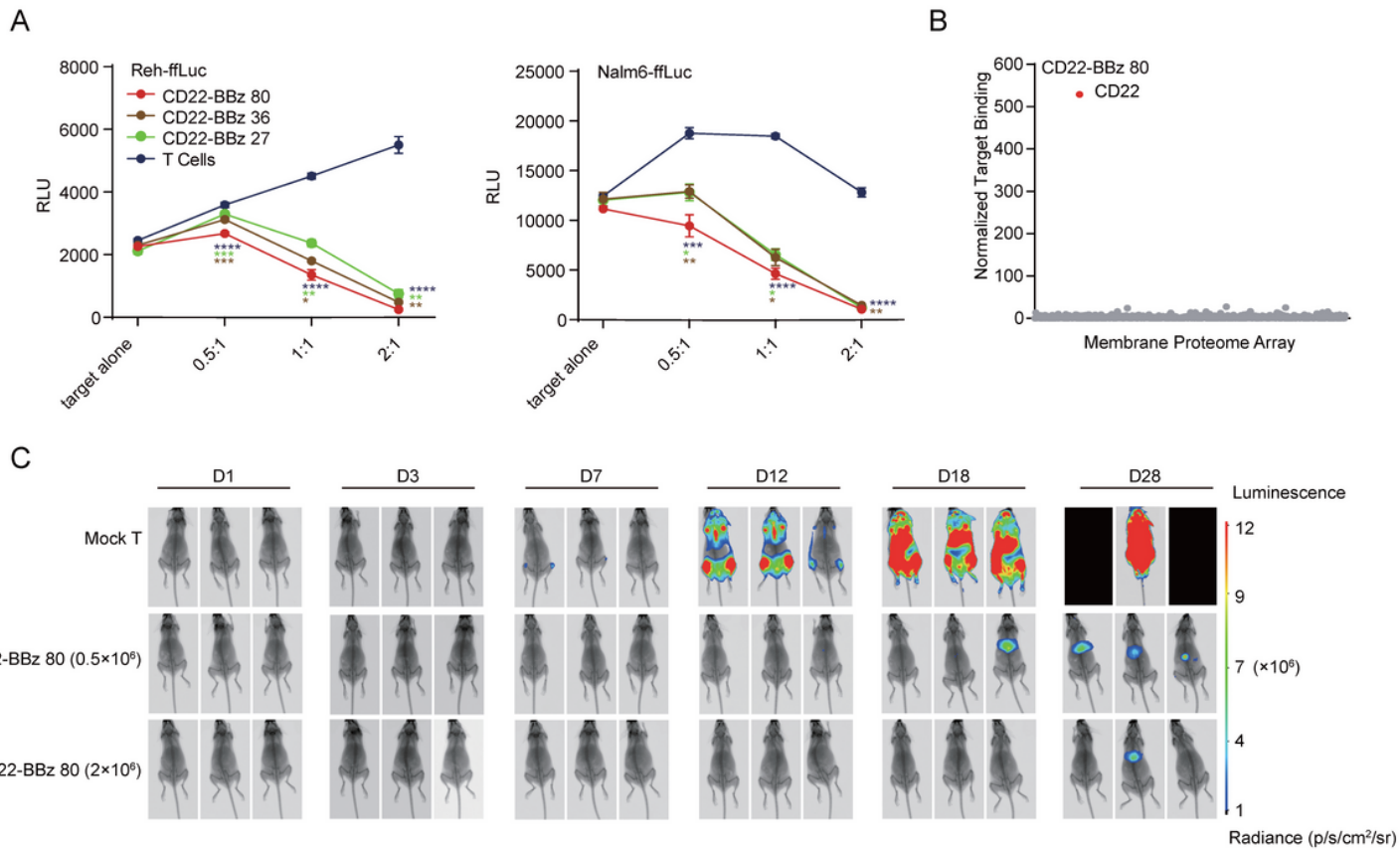


Figure 3

Figure 3

In vitro and in vivo evaluation of different CD22-BBz variants a, Cytolytic effects of specific CD22-BBz T cell clones against Nalm6 and Reh cells during co-culturing in triplicates at E:T ratios of 2:1, 1:1, 0.5:1 and 0:1. % specific lysis = (spontaneous relative light unit (RLU) – test RLU)/(spontaneous death RLU) × 100. A two-tailed, unpaired two-sample t-test was used for statistical analysis. The brown, green and blue asterisks indicate the comparison of the cytolytic effects of CD22-BBz 80 with that of CD22-BBz 36, CD22-BBz 27, or control T cells respectively. *P<0.05, **P<0.01, ***P<0.001, ****P<0.0001. b, Membrane proteome array for CD22-BBz 80. c, Xenograft model demonstrating the in vivo activity of CD22-CARFH80 T cells at indicated doses or mock-transduced T cells intravenously administered 2 days after Nalm6-Luc cell implantation. Tumor growth in each mouse was evaluated by measuring the photon using Bruker imaging system. The data are representative of at least 2 independent experiments with similar results.

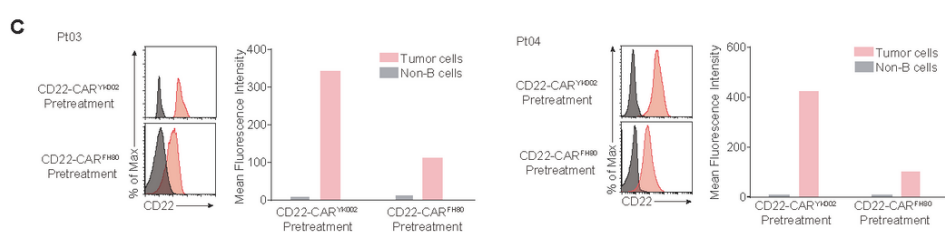
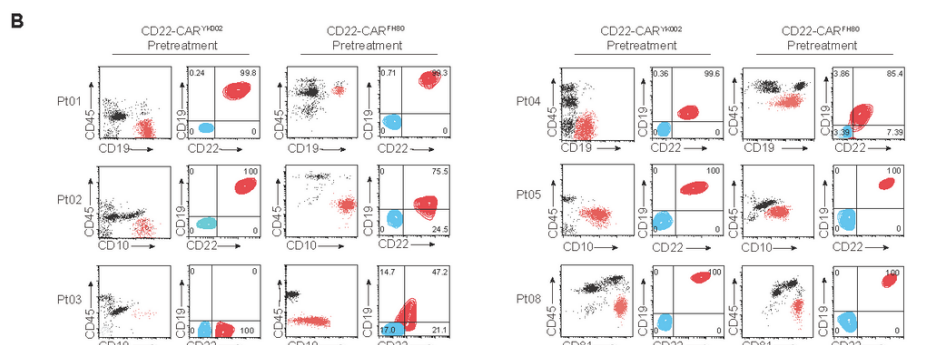
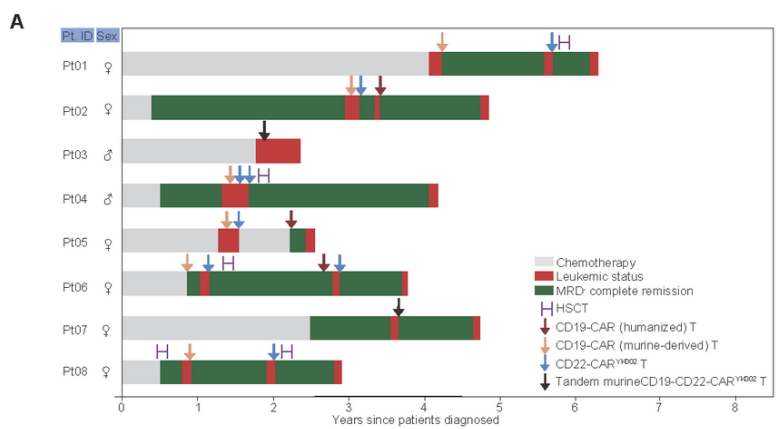
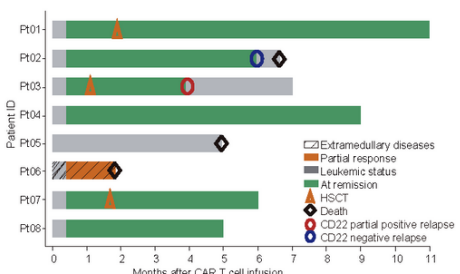


Figure 4

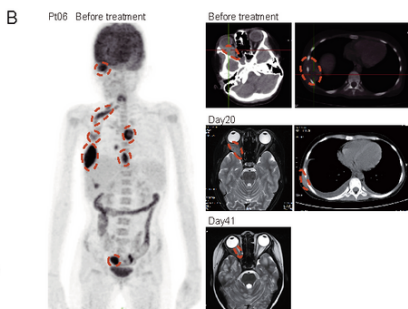
Figure 4

Treatment history, change of CD19/CD22 expression in 8 patients before enrolling in CD22-CARFH80 therapy a, Swimmer plot illustrating the treatment history of CD22-CARFH80 T clinical trial enrolled patients with B-ALL. Arrows indicate CAR T therapy. Patient number are shown to the left of the y axis. MRD, minimal residual disease; HSCT, allogeneic hematopoietic stem cell transplantation. b, Dot plots showing the proportions of blasts (red) and non-tumor cells (black) among all mononuclear cells from patients at indicated time points, and contour plots showing CD22 and CD19 expression on blasts (red) before CD22-CARYK002 and CD22-CARFH80 T cell therapy, determined by flow cytometry with a population of CD22-negative non-B cells with similar cell size in the same staining tube (blue) as negative control for evaluating CD22 expression level. The blasts were defined based on the combined analysis of multiple makers. The number represents the proportion of blasts (red) in the four quadrants. c, Histogram and mean fluorescence intensity of CD22 cell-surface expression in patient 03 and 04.

A



B



C

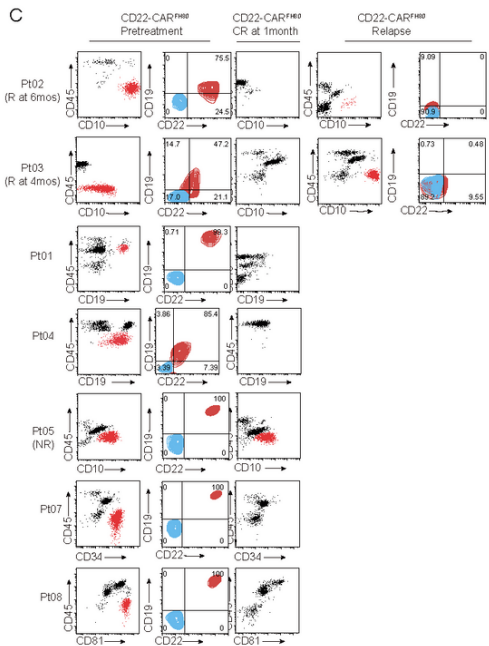
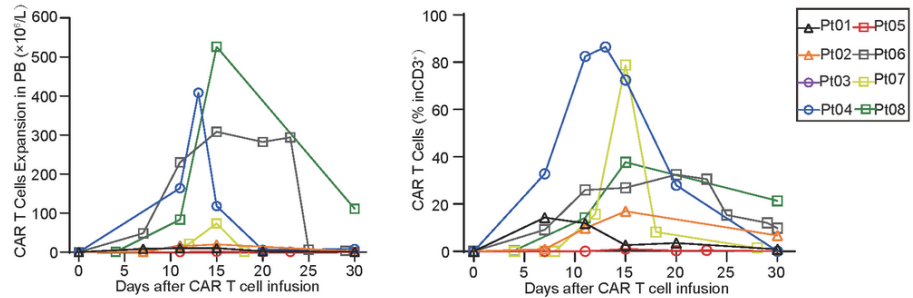


Figure 5

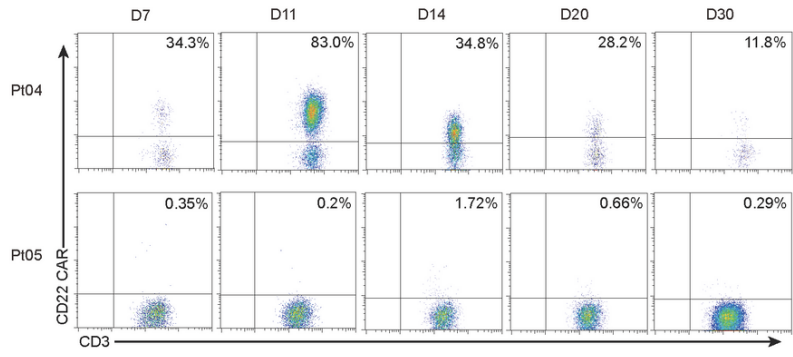
Figure 5

Clinical response and change of CD22 expression in response to CD22-CARFH80 T cell therapy a, Swimmer plot showing the clinical responses, response duration and outcome in individual patients treated with CD22-CARFH80 T cells. HSCT, hematopoietic stem cell transplantation. b, Images showing the retreatment extramedullary disease detected by Position Emission Tomography (PET), the reduction of intracranial mass detected by Magnetic Resonance Imaging (MRI), and the reduction of chest wall mass detected by Computed Tomography (CT) during CAR T cell treatment in patient 6. Red dotted circle indicates the border of a leukemia mass. c, Dot plots showing the proportions of blasts (red) and non-tumor cells (black) among all mononuclear cells from patients at indicated time points, and contour plots showing CD22 and CD19 expression on blasts (red) before and after CD22-CARFH80 T cell therapy, determined by flow cytometry with a population of CD22-negative non-B cells with similar cell size in the same staining tube (blue) as negative control for evaluating CD22 expression level. The blasts were defined based on the combined analysis of multiple makers. The numbers in the plot indicate the proportion of blasts in the four quadrants.

A



B



C

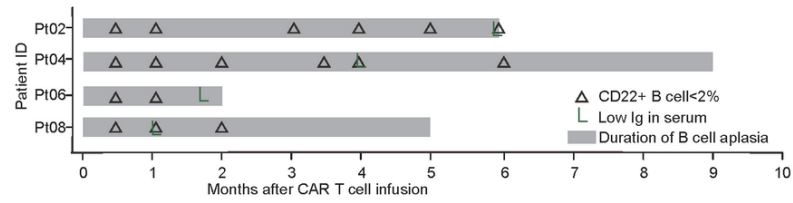
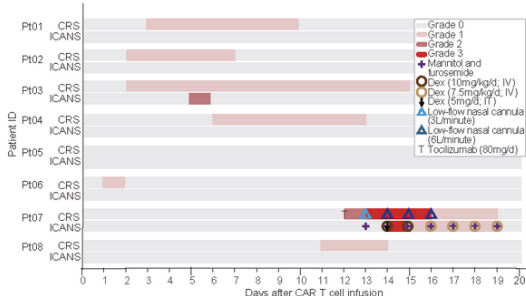


Figure 6

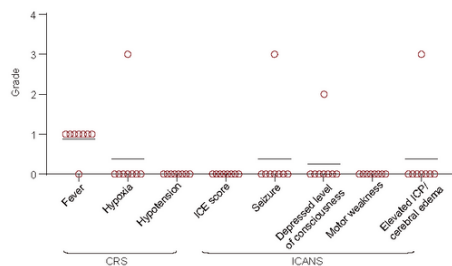
Figure 6

Efficient expansion of CD22-CARFH80 T cells in peripheral blood a, Absolute number of CAR T cells (left panel) and the percentage of CAR T cells among CD3 $^{+}$ T cells (right panel) in the peripheral blood of 8 patients who received CD22-CARFH80 T cell therapy. b, Representative dot plot, detected by flow cytometry, showing the presence of CD22-CARFH80 T cells among CD3 $^{+}$ T cells in the peripheral blood of two patients, including Pt 4 who achieved complete remission and Pt 5 who did not respond to the therapy. c, Swimmer plot showing the duration of B cell aplasia in bone marrow and hypogammaglobulinemia in 4 patients who achieved complete remission but received no further treatments. Serum immunoglobulins and bone marrow non-malignant B cells was determined by immunoturbidimetry and flow cytometry respectively.

A



B



C

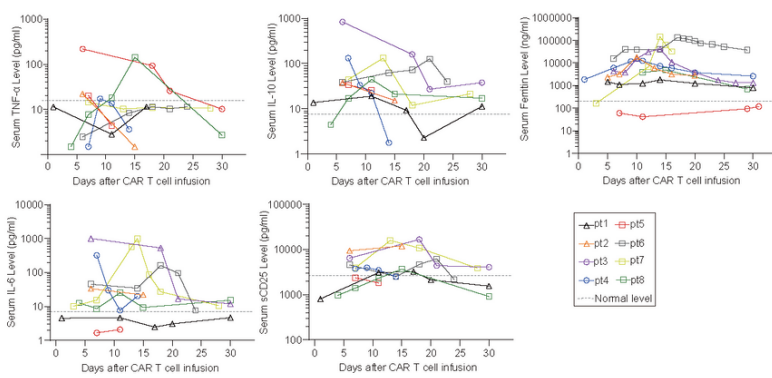


Figure 7

Figure 7

Adverse events, and elevation in serum cytokine levels after CD22-CARFH80 T cell infusion a, Swimmer plot showing the grade, duration and management CRS and ICANS in each patient. Color in the swimmer lane indicate the existence of a specific grade of CRS or ICANS on specific time point during CAR T cell treatment. IT, intrathecal injection; IV, intravenous injection; CRS, Cytokine-release syndrome; ICANS, immune effector cell-associated neurotoxicity syndrome. b, Symptoms of CRS and ICANS in individual patients during CD22-CARFH80 T cell therapy. Horizontal lines indicate mean values of the grade of specific symptoms. c, Kinetics of serum cytokines indicative of systemic inflammation in individual patients after CAR T cell infusion, as determined by Quantikine enzyme-linked immunosorbent or chemiluminescence microparticle immunoassay. Dotted horizontal lines indicate normal upper limit for specific cytokines.

Supplementary Files

This is a list of supplementary files associated with this preprint. Click to download.

- [TanYetalSupplementalMaterials.pdf](#)